Experimental validation of a multiple model predictive control for waste heat recovery organic Rankine cycle systems

Andres Hernandez[1], Fredy Ruiz[2], Sergei Gusev[4], Robin De Keyser[3,5], Sylvain Quoilin[1], Vincent Lemort[1]

Abstract

Waste heat recovery systems are today considered as a valuable solution to increase energy efficiency of industrial applications and heavy-duty vehicles, as it uses a thermodynamic organic Rankine cycle system to recover the heat losses to produce electrical or mechanical power. Optimal performance of such machines is often achieved at conditions where complex time-varying nonlinear dynamics are encountered, making the automatic control strategy a fundamental element to maximise the energy efficiency. In this paper the development of a multiple model predictive controller suitable for industrial implementation is presented, and its effectiveness is experimentally validated for the task of maximising output power of a 11 kW_{el} small-scale ORC power unit used in a waste heat recovery application. The main advantage of the proposed controller is the possibility to use different model structures to describe local dynamics without increasing complexity of the optimisation problem. Additionally, experimental results illustrate that the entire operating range of the system might be classified in two regions, a quasi-linear and a highly nonlinear region for 'high' and 'low' superheating degrees respectively. Closed-loops tests lead to the conclusion that a single linear model predictive controller might only be used under suboptimal operation of low power production (on the quasi-linear region for 'high' superheating), otherwise leading to poor performance or even instability. Alternatively, the proposed strategy keeps the cycle stable over the entire range of conditions and allows to increase the net electrical energy produced by at least 6%, even under drastic waste heat source variations, when operating closer to the minimum allowed superheating degree.

Keywords:
Multiple-Model Predictive Control, Organic Rankine Cycle, Energy efficiency, Waste heat recovery

1. Introduction

Energy efficiency is a major concern today as it opens the possibility to create a positive environmental and economic impact. From the different possibilities available, technologies able to recover heat at low temperatures are considered as an attractive solution as revealed by recent studies [1]. Among the different options the Organic Rankine Cycle (ORC) system stands out as a suitable and attractive solution for converting low temperature waste heat into electrical energy [2], it has been actively used in both research and industry for its reliability and cost-effectiveness [3].

While systems at power capacities in the range from hundreds kW_{el} to a few MW_{el} can be considered at a mature stage [4], the case of small-scale waste heat recovery (WHR) applications is still under development [5, 6]. Though great potential is expected once a better performance of the control unit for this system is achieved [7, 8], the highly fluctuating nature of the heat source (temperature and mass flow) makes WHR applications a challenging task [9], due mainly to heat exchanger dynamics [10, 11].

In order to make this technology a viable commercial solution, recent research has been focusing on optimising the performance of small ORC units adopting multi-objective optimisation for the design stage [12, 13], dynamic modelling to investigate the system dynamics [14, 15, 16] and to test control strategies during transient conditions [17, 18, 19, 20], thus encountering that in order to achieve the desired optimal performance control plays a major role [21].

The main challenges for the control strategy of ORC systems are: to keep the cycle in a safe condition during operation and to maximise the net energy production [11, 22]. On one hand, safe operation of the ORC unit is important as it allows a longer life expectancy in all components, this can be achieved by ensuring the vapour state at the inlet of the expander machine, i.e., an accurate regulation of the evaporator superheating. Note that displacement machines can handle droplets of liquid during the expansion, however this condition should be avoided in order to maximise the efficiency [23]. Additionally, the high pressure should also be limited using a by-pass valve and to prevent cavitation of the pump, as it would decrease the mass flow rate and consequently produce hot spots in the evaporator. On

[1]University of Liege, Energy Systems Research Unit, Thermodynamics laboratory, Campus du Sart Tilman B49, 4000 Liege, Belgium. *Corresponding author: jahernandez@uliege.be*
[2]Dipartimento di Elettronica, Informazione e Bioingegneria, Politecnico di Milano, Milan, Italy.
[3]Ghent University, Department of Electrical energy, Metals, Mechanical Constructions and Systems, DySc research group on Dynamical Systems and Control, Technologiepark 125, 9052 Ghent, Belgium.
[4]Ghent University, Department of Green Chemistry and Technology, Graaf Karel De Goedelaan 5, 8500 Kortrijk, Belgium.
[5]EEDT Decision and Control, Flanders Make, 9052 Ghent, Belgium

the other hand to maximise the output power the evaporating pressure represents the most relevant controlled variable [5, 24]. When two degrees of freedom are available i.e., pump and expander speed, controlling both superheating degree and evaporating pressure is often preferred. However, when the objective is to use only one degree of freedom, the control is limited to accurately regulate the superheating degree. Although, the control design is simplified considering the number of manipulated and controlled variables, it still remains as a challenging problem [21, 25].

The highly nonlinear relationship existing between rotational pump speed and superheating degree [26, 27], becomes an even more challenging situation due to the intrinsic fluctuating nature of the waste heat [16, 28], taking the system into a different operating condition, thus making possible to refer to this system as not only nonlinear but time-varying. Consequently a proper control system to operate the power machine safely and efficiently requires some kind of adaptive law [21], as reported in simulation studies in [29] where a gain-scheduling PID control strategy is proposed, together with a multiple model predictive control with explicit formulation in [30] and based on Generalized Predictive Control with recursive least-square formulation for model adaptation in [31]. Since the main interest is to maximise energy production, an optimal control problem with constraints is formulated as reported in [32] for an application of ORC for vehicles. A more recent study with a comparative analysis of power optimization for ORC systems is encountered in [33], showing the benefits for implementing dynamic programming and nonlinear model predictive control, as they outperforms PID strategies by 9.9%, and the implementation of nonlinear model predictive control with economic objective function in [34].

At the best of our knowledge few experimental works related to control system evaluation for ORC have been reported, and the work available has been focused on vehicles applications. Thus experimental tests include the development of a nonlinear model predictive control in [19], the comparison between PID and a multiple model MPC for superheating control in [35], the comparison between performance achieved with linear and nonlinear MPC in [36], and the implementation of gain-scheduling and a Linear Quadratic Regulator (LQR) in [37]. A complete review on modeling and control design is presented in [11]. A common frame for those studies is the use of models obtained from physical principles, while the number of actuators and control strategy vary depending on the specific configuration i.e., if an expander or turbine, and by-pass valves are employed [21]. However, it is encountered that more than one degree of freedom is more convenient for vehicle applications due to the system fast dynamics, given also for the smaller size of heat exchanger, and the larger and more drastic waste heat fluctuations compared to the industrial scenario [22].

A trend on the use of model-based strategies is encountered, including predictive algorithms to better anticipate waste-heat source variations and to optimise the power production during operation while respecting system constraints [38, 39]. Model predictive control (MPC) is a mature technology and has become the standard approach for implementing constrained, multivariable control strategies in the process industries today [40, 41]. MPC provides an integrated solution for controlling systems with interacting variables, complex dynamics, and constraints [42]. An important aspect in MPC refers to the modelling part, while the model may be linear or nonlinear, linear MPC is still widely used in the majority of industrial applications [43], and usually the model is identified using data generated from a dedicated plant test. Since real plants are inherently nonlinear, a possible choice to deal with nonlinearity consists in the use of several linear models which combined could extend the operating range of the controller.

In this work the contribution lies in the experimental validation of a proposed constrained multiple-model predictive control using one degree of freedom (i.e., pump speed as actuator) for controlling superheating degree. Transfer function models are obtained from experimental data, thus avoiding the difficulty encountered when developing models from physical principles as considered in other studies [32, 37]. A Bayesian probabilistic weighting scheme is considered for model selection. It must be highlighted that the proposed methodology guarantees that the complexity of the control law does not augment with number of active models detected by the Bayesian scheme, which represents an important advantage for implementation issues. Moreover, the order of each local transfer function can be chosen independently, not limited to rigid structures such as First order plus dead time (FOPTD) as in other studies [44, 45, 30, 31], thus allowing to more precisely describe complex dynamics encountered at low super heating degree. The control strategy here developed does not require the usage of state estimators as in [32], thus facilitating its implementation on hardware with limited computation capacity and the understanding of the tuning by process operators. The tracking and disturbance rejection performance of the proposed MMPC is experimentally evaluated for the accurate superheating regulation of an $11\,\mathrm{kW_{el}}$ organic Rankine cycle (ORC) waste heat recovery power unit using R245FA as working fluid, which exhibits time-varying nonlinear dynamics in its point of maximum energy efficiency [24, 29, 39]. It is besides illustrated that a single model predictive control is not sufficient to operate the system due to variability of the heat source conditions, a natural state of waste heat recovery applications in both industry and automotive, that can lead the system to operating conditions where stronger nonlinearities are encountered. The interested reader is referred to [46] where an overview of the challenges of waste heat thermal power fluctuations for industry and automotive are described for several practical applications..

The paper is structured as follows. In section 2 the small-scale organic Rankine cycle (ORC) power unit for waste-heat recovery is fully described, including experimental results illustrating the nonlinear time-varying characteristic of the system and the model bank design. Next in section 3 the mathematical description of the proposed Multiple-Model MPC strategy is presented. Followed by section 4 where the performance of the proposed strategy to enhance the power production of this challenging system is experimentally evaluated. Finally, a conclusion section summarizes the main outcomes of this contribution.

2. Small-scale ORC waste heat recovery experimental study

In this section is presented the description of the ORC pilot plant and the experimental tests to illustrate its nonlinear dynamics.

2.1. The organic Rankine cycle experimental facility

The system considered is the small-scale organic Rankine cycle (ORC) unit with schematic layout presented in Fig. 1. The system based on a cycle with recuperator and R245fa as working fluid, has a nominal power of 11 kW_{el}. A twin-screw expander drives a synchronous permanent magnet generator connected to the electric grid through a four-quadrant inverter, which allows varying the generator rotational speed (N_{exp}). Although the maximum expander rotation speed is 10000 rpm, during the experiments performed in this paper, the generator rotating speed is kept constant at 5000 rpm, without affecting the generality of the obtained results. The circulating pump (N_{pp}) is a vertical variable speed 14-stage centrifugal pump with a maximum pressure of 14 bar and 2.2 kW_{el} nominal power.

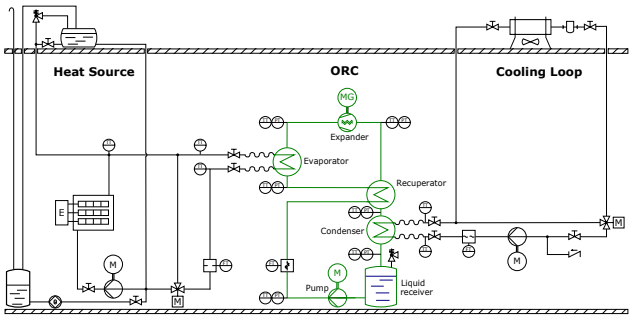

Figure 1: Schematic layout of the pilot plant available at Ghent University, campus Kortrijk (Belgium)

Starting from the bottom of the ORC installation highlighted in green in Fig. 1, it is possible to recognize the liquid receiver installed at the outlet of the condenser where the fluid is collected in saturated liquid condition. From the receiver outlet, the fluid typically slightly subcooled is pumped through the recuperator cold side, and the evaporator, where it is heated up - by the waste heat - to superheated vapour, reaching its maximum temperature at the evaporator outlet. The fluid, after being expanded in the volumetric machine, enters the recuperator hot side, and then it flows into the condenser to close the cycle.

In order to operate the machine close to optimal conditions, superheating degree plays a major role [5]. The superheating is defined as:

$$\Delta T_{sh} = T_{exp,su} - T_{sat,ev} \tag{1}$$

where $T_{exp,su}$ is the temperature measured at the expander inlet and $T_{sat,ev}$ the evaporating temperature, corresponding to the temperature at which the fluid undergoes the phase transition from saturated liquid to saturated vapour at the evaporating pressure $P_{sat,ev}$, assuming no pressure drop in the evaporator:

$$T_{sat,ev} = f(P_{sat,ev}) \tag{2}$$

where f corresponds to a nonlinear function that correlates the pressure for the refrigerant R245fa [5].

The main terms to assess the performance of the ORC system are the net output power and the cycle efficiency which are defined as:

$$\dot{W}_{net} = \dot{W}_{exp} - \dot{W}_{pump} \tag{3}$$

$$\eta_{cycle} = \frac{\dot{W}_{net}}{\dot{Q}_{in,ORC}} \tag{4}$$

where $\dot{W}_{exp}$ is the expander electrical power, $\dot{W}_{pump}$ is the pump electrical power and $\dot{Q}_{in,ORC}$ is the thermal (waste heat) power supplied to the ORC system in the evaporator.

In order to compare the developed methodologies and control strategies, it is important to guarantee that all experiments are performed in similar and repeatable conditions. This means that controllers for the secondary loops (i.e., heat source and cooling loop) are necessary. The interested reader is referred to [15, 39] for further details about instrumentation, acquisition system and secondary loops control design for the pilot plant.

2.2. Illustrating the ORC system nonlinearity

In order to illustrate the presence of a nonlinearity in the system, the static characteristic obtained from experimental tests is represented in Fig. 2, where superheating ΔT_{sh}, evaporating temperature $T_{sat,ev}$ and electric power produced in the expander W_{exp} are plotted as a function of pump speed N_{pp}, for the 4 pairs of extreme conditions of the waste heat source for temperature $T_{hf} = \{110-120\}$ °C and mass flow rate $\dot{m}_{hf} = \{1.3-2.1\}$ kg/s.

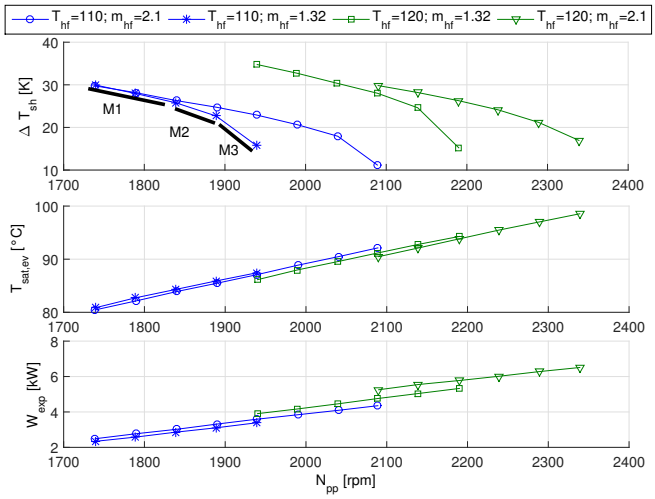

Figure 2: Static characteristics of the system for superheating ΔT_{sh}, evaporating temperature $T_{sat,ev}$, and expander electrical power $\dot{W}_{exp}$, obtained experimentally for different heat source conditions T_{hf} and $\dot{m}_{hf}$. Black width line represents the minimum number of local linear models (M_x) required to approximate the nonlinearity present for superheating.

Notice that from the gain point of view, it is possible to conclude that $T_{sat,ev}$ and $\dot{W}_{exp}$ are fairly linear, when observing the static characteristic representation, whilst the challenge appears for superheating ΔT_{sh}, as the gain change is nonlinear. Making a first rough approximation, one could observe an inflection

point or 'elbow' point, where a drastic change in superheating gain occurs. The superheating degree is fairly linear for 'high' superheating values above the elbow point, and quickly drops becoming highly nonlinear for 'low' superheating values below the elbow point.

Considering the test in Fig. 2 where $T_{hf} = 110\,^{\circ}\mathrm{C}$ and $\dot{m}_{hf} = 2.1\,\mathrm{kg/s}$, it is possible to observe that the elbow point appears at $\Delta T_{sh} = 20\,\mathrm{K}$ corresponding to pump speed $N_{pp} = 1980\,\mathrm{rpm}$, meaning that the highly nonlinear region starts for values below that superheating degree. On the other hand, for the case of $\dot{m}_{hf} = 1.3\,\mathrm{kg/s}$, the elbow point can be approximated at $\Delta T_{sh} = 25\,\mathrm{K}$ for $N_{pp} = 1850\,\mathrm{rpm}$, therefore concluding that the highly nonlinear region starts at higher superheating degree. This experiment leads to the conclusion that waste heat fluctuations might lead the system to other conditions where nonlinear region can be enlarged making more challenging the modelling and control tasks. Additionally, the gain changes can be quite significant as for the same pump speed e.g., $N_{pp} = 1940\,\mathrm{rpm}$ three different superheating values are observed $\{15, 24, 35\}\,\mathrm{K}$ when waste heat conditions change, thus producing a gain change (i.e., $gain = \Delta T_{sh}/N_{pp}$) of up to 233%.

The previous observation is in agreement with conclusions learned from other studies (e.g., [24, 39]), there exists a nonlinear relationship between rotational pump speed and superheating degree, where it is possible to observe that the 'elbow' or point where superheating nonlinearity becomes stronger changes for different the waste heat conditions i.e., mass flow rate and temperature. Therefore, to cover the entire range of conditions, models have to be identified at 'high' and 'low' superheating values, for the minimum and maximum expected variations of the heat source conditions.

One could define three regions (M_x for $x = 1, \ldots, 3$) which might be sufficient to obtain a linear approximation of the curvature change of superheating with the minimum number of linear models. Based on previous reasoning, it is then decided to consider at least three operating points (i.e., pump speed, N_{pp}) for each pair of heat source conditions (i.e., T_{hf} and $\dot{m}_{hf}$). Hence by considering the minimum and maximum heat source temperature and three mass flow rate values, a number of 18 testing conditions are obtained, as registered in Table 1 (Section 4). Note that only the maximum and minimum heat source temperature T_{hf} are chosen to perform the tests (i.e., $120\,^{\circ}\mathrm{C}$ and $110\,^{\circ}\mathrm{C}$), whilst three cases are selected for the mass flow rate in the heat source $\dot{m}_{hf}$ as the system nonlinearity is mainly triggered by this variable, as previously explored.

Based on the previous observations, where it is shown how the gain varies nonlinearly with the heat source and with the manipulated variable, system can be defined as nonlinear and time-varying, given the fluctuating nature of the waste heat. It is worthy to mention that gain changes are illustrated here for simplicity, nevertheless system exhibits nonlinear dynamics as well [24, 39], e.g., if approximate to a first order model, the time constant might vary up to 10 times.

3. The proposed Multiple-Model Predictive Control

The multiple model control strategy is a mathematically attractive and practically viable method, to improve the tracking performance and disturbance rejection capabilities of a system with strong nonlinearity and/or varying operating conditions [44]. It has appeared as a solution to avoid nonlinear models which might lead to complex optimisation problems, which are no longer convex and where convergence to the global optimum is not always guaranteed [47]. Suboptimal solutions exist to deal with the system nonlinearities using the MPC framework, where the nonlinear model is used for prediction while a linear perturbation model is used for the optimisation iterations, thus resulting in a convex optimisation problem. Examples of such approaches include the nonlinear quadratic Dynamic Matrix Control (NL-QDMC) [48, 49, 50] and the Nonlinear Extended Prediction Self-Adaptive Control (NEPSAC) [51, 52]. The interested reader is referred to [41, 47], where a complete review of NMPC algorithms is reported. Previous methodologies require a nonlinear model of the system, either developed from physical principles or by black-box identification. Main drawbacks for those approaches are the difficulty to build and identify parameters for the former case, and the large amount of required data in the latter.

In this section a pragmatic approach, which can be more easily accepted and adopted in industry, consists in using a multiple linear model strategy. The methodology applied to the MPC concept is depicted in Fig. 3, where three main components are recognized, namely the model bank, weight computation and predictive control optimisation. Note that $y(t)$ represents the controlled variable (superheating ΔT_{sh}) and $u(t)$ the manipullated variable (pump speed N_{pp}).

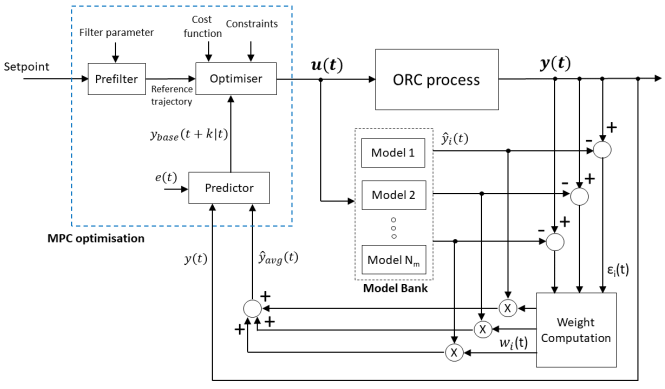

Figure 3: Schematic representation of the principles of the proposed Multiple-Model MPC strategy.

The methodology relies on the use of a bank of linear models to describe the dynamic behaviour of the plant over a wide operating range, where a recursive Bayesian scheme assigns weights to each prediction. The combined-weighted prediction is then used to compute the optimal control action. The concepts of the algorithm originally developed for the Multiple-Model Dynamic Matrix Control in [44], inspires the development of the Multiple-Model Prediction control here proposed, using as

MPC framework the Extended Prediction Self-Adaptive Control (EPSAC) approach, originally introduced in [53, 54] and more recently investigated in [52, 55, 56]. The proposed industrial MMPC controller takes advantages of the filtering techniques used for prediction, allowing to use different model structures in the bank without an increasing complexity of the optimisation problem, thus making it suitable for implementation on hardware with limited capacity. Moreover, the performance of the algorithm and the tuning requirements are experimentally validated when applying it to a nonlinear time-varying WHR-ORC power system.

3.1. Control objective

The objective of the MPC strategy is to find the input sequence $\delta u(t+k|t)$ that minimizes a given cost function, based on a desired output trajectory over a prediction horizon N_p subject to system dynamics. This cost function considers the errors between the predicted model outputs $y(t+k|t)$ and the reference trajectory $r(t+k|t)$, leading to the following optimisation problem:

$$\begin{aligned} \min_{U\in\mathbb{R}^{N_c}} & \sum_{k=1}^{N_p}[r(t+k|t)-y(t+k|t)]^2+\lambda\sum_{k=0}^{N_c-1}[\delta u(t+k|t)]^2 \\ \text{subject to:} \quad & y(t+k)=f(y,u) \\ & y_{min}\le y(t)\le y_{max} \\ & u_{min}\le u(t)\le u_{max} \\ & \Delta u_{min}\le u(t)-u(t-1)\le \Delta u_{max} \end{aligned} \tag{5}$$

where the prediction horizon, N_p is an optimisation parameter which influences the closed-loop dynamics, (i.e., a shorter prediction will generally produce a faster response with a larger control effort). The control horizon N_c refers to the number of control moves, using a shorter control horizon than the prediction horizon ($Nc \le Np$), has a positive impact on the closed-loop stability by reducing the degrees of freedom in the control input [57]. Further details about N_p and N_c are given in section 3.4. An additional parameter to adjust the closed-loop speed is the weighting factor λ, whereas the first term of the cost function minimizes the tracking error, the second term focuses on the magnitude of the control increment, i.e., a large value of λ penalizes the control action.

The desired reference trajectory, $r(t+k|t)$, is here chosen as a 1st-order trajectory

$$r(t+k|t)=\alpha r(t+k-1|t)+(1-\alpha)w(t+k|t)$$

for $k=1,\ldots,N_p$ with initialization $r(t|t)=y(t)$. The signal $w(t)$ represents the setpoint and alpha ($0\le\alpha\le 1$) is a design parameter to tune the MPC performance [57].

In general, the system prediction expressed in matrix form $\mathbf{Y}=[y(t+1|t)\ldots y(t+N_p|t)]^T$, is calculated by

$$\mathbf{Y}=\overline{\mathbf{Y}}+\mathbf{G}\,\mathbf{U} \tag{6}$$

where the first term $\overline{\mathbf{Y}}$ corresponds to the base (or free) response and the second $\mathbf{G}\,\mathbf{U}$ to the optimising (or forced) response [42], with the control actions represented in matrix form $\mathbf{U}=\delta u(t|t),\ldots,\delta u(t+N_c-1|t)$. More details are given in the next subsection when describing the output predictor. Thus, the control law is obtained by minimising the cost function through an optimiser. Next by using equation (6) as a way to express predictions, the cost function (5) can be rewritten in its matrix form:

$$[(\mathbf{R}-\overline{\mathbf{Y}})-\mathbf{G}\,\mathbf{U}]^T[(\mathbf{R}-\overline{\mathbf{Y}})-\mathbf{G}\,\mathbf{U}]+\lambda\,\mathbf{U}^{\mathbf{T}}\mathbf{U} \tag{7}$$

Due to system constraints, there is no direct analytical solution resulting in a nonlinear optimisation problem. Nevertheless, as the cost function (5) is quadratic with linear constraints with respect to decision variables $\mathbf{U}$, then the minimization problem can be solved by a Quadratic Programming (QP) algorithm [42] as follows

$$\begin{aligned} & \mathbf{U}^T\Phi\mathbf{U}+2\Theta^T\mathbf{U}+c \\ & subject\,to: \\ & M\cdot\mathbf{U}\le N \end{aligned} \tag{8}$$

resulting for the SISO (Single Input Single Output) case in the Φ and Θ matrices:

$$\begin{aligned} \Phi &= \mathbf{G}^T\mathbf{G}+\lambda I \\ \Theta &= -\mathbf{G}^T(\mathbf{R}-\overline{\mathbf{Y}}) \\ c &= (\mathbf{R}-\overline{\mathbf{Y}})^T(\mathbf{R}-\overline{\mathbf{Y}}) \end{aligned} \tag{9}$$

In equation (7), the first element of the decision variable $\mathbf{U}$ obtained from the quadratic programming method, is the control increment that will be applied to the system in the next sampling time $(t+1)$.

In this work the Hildreth QP algorithm to solve (8) is implemented to ensure numerical robustness and stability of the solution, as it is particularly suitable to recover from ill-conditioned problems [58].

3.2. The model bank

The model bank consists of N_m models identified for different operating regions and/or waste heat source conditions. The number of models is based on the range of operability desired and the allowable maximum distance between adjacent models [44].

For the method to be used, it is important to define a model for unbiased prediction in steady-state [44], since the proper choice of the weights in the Bayesian scheme depends on the model residuals $\varepsilon_{i,k}$, this can be achieved using the popular CARIMA-model:

$$A_i(q^{-1})\hat{y}_i(t)=B_i(q^{-1})u(t)+\frac{C(q^{-1})}{\Delta}e(t) \tag{10}$$

where polynomials A, B, C are represented using the backward shift operator q^{-1}, i.e., $q^{-n}p(t)=p(t-n)$, $p(t)$ being a time-dependent signal and t denoting the discrete-time index ($t=0,1,2,...$). And with $\Delta=1-q^{-1}$ and $i=1,\ldots,N_m$. Which after making some manipulations leads to:

$$A_i(q^{-1})\Delta\hat{y}_i(t)=B_i(q^{-1})\Delta u(t)+C(q^{-1})e(t) \tag{11}$$

Notice that in steady-state the last term in previous equation vanishes $C(q^{-1})e(t) \approxeq 0$, because $e(t)$ is white noise (a zero mean random variable); leading to the incremental form of the prediction model:

$$[A_i(q^{-1})\Delta]\hat{y}_i(t) = B_i(q^{-1})[\Delta u(t)] \tag{12}$$

By defining $\tilde{A}_i(q^{-1}) = A_i(q^{-1})\Delta = 1 + \tilde{a}_1 q^{-1} \ldots + \tilde{a}_{na} q^{-n_a}$, the prediction based on output and input increments is obtained:

$$[\tilde{A}_i(q^{-1})]\hat{y}_i(t) = B_i(q^{-1})[\Delta u(t)] \tag{13}$$

Leading to the prediction model:

$$\begin{aligned} \hat{y}_i(t) &= -\tilde{a}_1\hat{y}_i(t-1) - \ldots - \tilde{a}_{na}\hat{y}_i(t-na) \\ &+ b_1\Delta u(t) + b_2\Delta u(t-1) + \ldots + b_{nb}\Delta u(t-nb) \end{aligned} \tag{14}$$

3.3. The recursive Bayesian weighting scheme

The model selection relies on a probabilistic approach, in which it is evaluated what is the likelihood of a model output to be equivalent to the actual plant output, the evaluation and later computation of the weights is based on the past history of the model residuals, i.e., error between the actual plant output and the models prediction $\varepsilon_i(k) = y(k) - \hat{y}_i(k)$. The weight computation for the kth step and i^{th} model is:

$$w_{i,k} = \begin{cases} \dfrac{P_{i,k}}{\sum_{j=1}^{N_m} P_{j,k}} & \text{for} \quad P_{i,k} > \psi \\ 0 & \text{for} \quad P_{i,k} \leq \psi \end{cases} \tag{15}$$

where $P_{i,k}$ is the probability of the ith model in the bank being the true model of the plant. Since it is very likely that a model that initially does poorly at predicting the plant output, may be needed later due to a disturbance or change in operating conditions, it is critical that all models are available for future selection. Hence, to keep all models alive in the bank, a small probability cut-off, $\psi = N_m^{-1}$, is assigned to each of the models when $P_i < \psi$ so their probabilities never go to zero. The scheme results in the following weights normalization:

$$w_{i,k} \in [0,1] \quad \text{such that} \quad \sum_{i=1}^{N_m} w_{i,k} = 1, \forall k;$$

Therefore, allowing to select a unique prediction model, if present in the bank. When a single model does not describe the plant, the scheme provides an interpolation between models by assigning fractional weights to each model, by using the tuning parameter as discussed next.

The probabilities are assumed to be stochastic in nature and Gaussian. The recursive Bayes theorem for the kth step and i^{th} model is

$$P_{i,k} = \frac{exp\left(-\frac{1}{2}\varepsilon_{i,k}^T \mathbf{K}\, \varepsilon_{i,k}\right) P_{i,k-1}}{\sum_{j=1}^{N_m} exp\left(-\frac{1}{2}\varepsilon_{j,k}^T \mathbf{K}\, \varepsilon_{j,k}\right) P_{j,k-1}} \tag{16}$$

where $\mathbf{K}$ is a diagonal matrix convergence tuning parameter, since the probability is computed considering a range of past values of the residuals. For notation convenience in the following we will only refer to K, which is the scalar parameter which multiplies a properly sized identity matrix $\mathbf{K} = K \cdot \mathbf{I}$, meaning that diagonal values in $\mathbf{K}$ are all equal. The K parameter is used to tune between: more blending of the models when large values are chosen for K or to converge to a single model if lower values for K are selected. Note that once the controller reaches and maintains a set point, further convergence of the model bank ceases.

Remark 1. *It can be seen from equation* (16) *that the probability calculation is recursive, and the probability at time instant k relies on the one calculated at previous time instant $k-1$. The algorithm allows to reject poor models exponentially fast, therefore allowing the use of a large number of models without deteriorating control performance or increasing substantially the computational effort.*

3.4. The output predictor

Conceptually and based on the superposition principle the output prediction $\{y(t+k|t),\, k = 1,\ldots,N_p\}$, can be obtained using the concepts of base (or free) and optimising (or forced) responses. Where it is established that the optimal control action $u(t)$ is the sum of an a priori defined basic control future scenario u_{base} and an optimising future control actions δu, such that

$$u(t+k|t) = u_{base}(t+k|t) + \delta u(t+k|t)$$

this concept is depicted in Fig. 4, where $u(t+k|t)$ is the optimal control input that we are looking for. It is a common practice to structure the future control scenario, thus reducing the degrees of freedom in the control vector $\{u(t+k|t),\, k = 0,\ldots,N_p - 1\}$. This is usually done through the control horizon (with $1 \leq N_c \leq N_p$) after which the (postulated) control strategy remains constant: $\{u(t+k|t) = u(t+N_c-1|t),\, k \geq N_c\}$, thus reducing the degrees of freedom from N_p to N_c. Structuring leads to simplified calculations and has generally a positive effect on robustness [52].

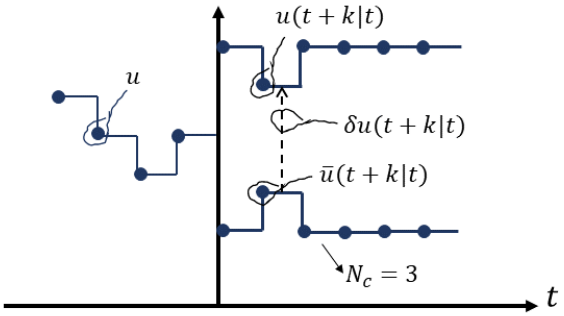

Figure 4: Concept of Base and Optimising control actions.

Using the model (14) recursively and considering the basic control scenario $\{u_{base}(t+k|t) = 0,\ k = 0,\ldots,N_p - 1\}$, valid for linear systems, it is possible to make a forward prediction

of the process output for each i model, i.e., $\hat{y}_i(t+k|t)$ for $k = 0,\ldots,N_p-1$.

Finally, the predicted average output can be obtained by multiplying the predicted trayectory for each model in the bank using (14) and the weights computed in (15) computed from the probability of each model to be the true model of the plant.

$$\hat{y}_{avg}(t+k|t) = \sum_{i=1}^{N_m} w_i(t)\hat{y}_i(t+k|t), \quad \text{for } k = 1,\ldots,N_p \tag{17}$$

Remark 2. *Notice that compared to other methods reported in literature for Multiple Model Predictive Control [30, 31, 44], the one here proposed takes the average of the trajectories rather than the average of the models, making possible to use and combine different model structures (orders of the transfer functions) in a straight forward manner. This result is of major importance for ORC systems, since different order transfer functions are required to properly describe the system dynamics at 'high' and 'low' superheating values as illustrated in Fig. 6 (section. 4).*

3.5. Treatment of modelling errors and disturbances

The modelling errors and disturbance rejection, are considered as coloured noise thus leading to the following disturbance model:

$$n(t) = \frac{C(q^{-1})}{D(q^{-1})}e(t) \tag{18}$$

with polynomials C, D represented using the backward shift operator q^{-1} and $e(t)$ uncorrelated white noise. The proposed algorithm uses filtering techniques as in EPSAC algorithm on [52], where correction is performed by first computing the difference between the actual plant output and the average prediction output:

$$n(t) = y(t) - \hat{y}_{avg}(t) \tag{19}$$

Using equation (18) it is possible to compute de filtered disturbance signal

$$n_f(t) = \frac{D(q^{-1})}{C(q^{-1})}n(t) \tag{20}$$

using previously stored values for n_f and n signals from the data base.

Furthermore by inspection of model (18) it is possible to note that the signal calculated $n_f(t)$ is a white noise signal, therefore concluding that $n_f(t) = e(t)$ [52]. Because white noise is by definition uncorrelated, its best prediction is the mean value, thus leading to:

$$n_f(t+k|t) \equiv 0, \quad k = 1,\ldots,N_p \tag{21}$$

Hence the best prediction of the disturbance is obtained from

$$n(t+k|t) = \frac{C(q^{-1})}{D(q^{-1})}n_f(t+k|t) \tag{22}$$

Using this procedure recursively with previous values in the database $(t-1,t-2,t-3,\ldots)$, leads to exactly the same solution as the alternative procedure - which is based on Diophantine equations, however the former is computationally inexpensive making of it an interesting solution for low capacity hardware implementations.

Finally the base response is then the sum of the average prediction plus the correction term:

$$y_{base}(t+k|t) = \hat{y}_{avg}(t+k|t) + n(t+k|t), \quad k = 1,\ldots,N_p \tag{23}$$

On the other hand the optimise response $y_{optimise,i}(t+k|t)$ for the ith model is the effect of the optimising control actions $\{\mathbf{U} = \delta u(t|t),\ldots,\delta u(t+N_c-1|t)\}$, in a control horizon N_c. Thus, the component $y_{optimise,i}$ can be expressed as the discrete-time convolution of U, the unit impulse response coefficients $h_1,\ldots,h_{N_p}$ and the unit step response coefficients $g_1,\ldots,g_{N_p}$ of the ith model as follows:

$$\begin{aligned} y_{optimise,i}(t+k|t) = h_k\delta u(t|t) + h_{k-1}\delta u(t+1|t) + \ldots \\ + g_{k-N_c+1}\delta u(t+N_c-1|t) \end{aligned} \tag{24}$$

using matrix notation previous result in (24) leads to:

$$\mathbf{Y}_{optimise,i} = \mathbf{G}_i \cdot \mathbf{U} \tag{25}$$

with:

$$\mathbf{G}_i = \begin{bmatrix} h_1 & 0 & \ldots & g_{1-N_c+1} \\ h_2 & h_1 & \ldots & \ldots \\ \ldots & \ldots & \ldots & \ldots \\ h_{N_p} & h_{N_p-1} & \ldots & g_{N_p-N_c+1} \end{bmatrix} \tag{26}$$

Since the computation is not performed for a single i model, but for the combination of N_m models according to the probabilities previously computed, the average G matrix is calculated using weights from (15), leading to:

$$\mathbf{G}_{avg} = \sum_{i=1}^{N_m} w_i\mathbf{G}_i \tag{27}$$

In conclusion the optimisation problem (8) and (9) for the proposed MMPC algorithm must be solved considering

$$\mathbf{G} \equiv \mathbf{G}_{avg}$$

and:

$$\begin{aligned} \mathbf{Y} &= [y(t+1|t)\ldots y(t+N_p|t)]^T \\ \overline{\mathbf{Y}} &= [y_{base}(t+1|t)\ldots y_{base}(t+N_p|t)]^T \\ \mathbf{U} &= [\delta u(t|t)\ldots\delta u(t+N_c-1|t)]^T \\ \mathbf{R} &= [r(t+1|t)\ldots r(t+N_p|t)]^T \end{aligned} \tag{28}$$

Remark 3. *The latter result obtained in equations* (17) *and* (27) *is of major importance when considering implementation aspects, since the structure of the resulting optimisation problem is the same as in regular single model MPC approach disregarding the number of active models in the bank; i.e., the complexity of the optimisation problem does not increase with the number of active models in the bank.*

Algorithm 1 Procedure to obtain the optimal control sequence $u(t+k|t)$ for the proposed MMPC strategy

1: Measure superheating output $y(t)$, and compute the optimal reference trajectory $r(t+k|t)$.
2: Obtain $\hat{y}_i(t+k|t)$ for $k=1,\ldots,N_p$ and $i=1,\ldots,N_m$, using $U_{base}(t+k|t)=0,\ k=0,\ldots,N_p-1$.
3: Compute the Bayesian probability of each i model prediction to be equal to the plant output using equations (16) and (15).
4: Obtain the average future trajectory $\hat{Y}_{avg}(t+k|t)$ using equation (17).
5: Compute the correction trajectory to compensate for modelling errors and disturbances, first obtaining the current error from equation (19), and the noise filtered signal at time t using (20) and the previous values for n_f and n stored in the database.
6: Compute disturbance prediction from (22), considering $n_f(t+k|t)\equiv 0$ for $k=1,\ldots,N_p$ as it is equivalent to white noise.
7: Obtain $y_{base}(t+k|t)$ from equation (23).
8: Compute the average $\mathbf{G}$ matrix using (27).
9: Solve the quadratic programming (QP) problem (8) and (9) to obtain the optimal $\mathbf{U}$ sequence, with $\overline{\mathbf{Y}}=\mathbf{Y}_{base}$ from step 7 and $\mathbf{G}=\mathbf{G}_{avg}$ from step 8.
10: Compute the optimal control action $u(t+k|t)=u_{base}(t+k|t)+\delta u(t+k|t)$.
11: Apply only the first element from optimal control sequence obtained from step 10, i.e., $u(t)=u_{base}(t|t)+\delta u(t|t)$. Therefore pump speed $N_{pp}=u(t)$.
12: At next sample time $t+1$ repeat the complete procedure starting from step 1, applying only the first action from the new control sequence. This is the so-called *receding horizon principle*.

In order to summarize the complete procedure the algorithm to obtain the optimal control sequence $u(t+k|t)$ is summarized as follows:

The flow-chart of algorithm 1 for MMPC is depicted in Fig. 5.

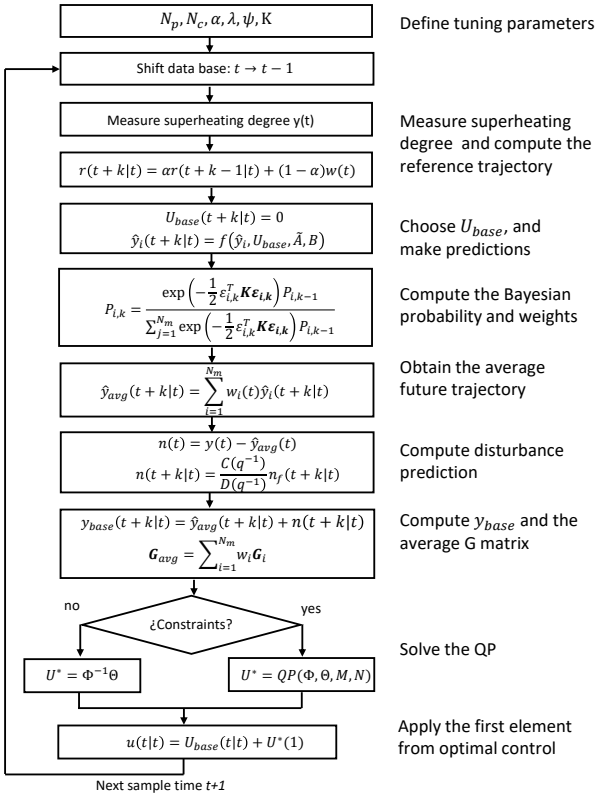

Figure 5: Concept of Base and Optimising control actions.

4. Experimental results and Discussion

In this section, we present some of the results to demonstrate the controller performance for superheating regulation.

4.1. Design of the model bank

Some step input variations in the pump speed are applied for the chosen operating points described in Table 1, in order to define a suitable input amplitude which produces a superheating variation of at least 2 K, in order to have a good signal-to-noise ratio (SNR). Furthermore, a sampling time $T_s=1$ s is chosen according to the smallest time constant observed after applying the step input.

The identification is performed in open-loop using a Pseudorandom Binary Sequence (PRBS) as excitation signal. The amplitude of the PRBS is the same as the one previously defined to achieve a desirable SNR; whilst the length is chosen as 10 times the step response settling time, in order to obtain

sufficient information for the identification procedure. Subsequently, transfer function models are obtained from the input-output experimental data using the prediction error method proposed in [59].

Table 1: Testing conditions of the identified bank of models.

Model	T_{hf} [°C]	$\dot{m}_{hf}$ [kg/s]	N_{pp} [rpm]	ΔT_{sh} [K]
1	120.0	2.10	1999	34.47
2	120.0	2.10	2148	25.49
3	120.0	2.09	2199	20.47
4	120.0	2.09	2219	15.06
5	**120.0**	**1.70**	**1999**	**33.54**
6	120.0	1.70	2069	24.90
7	120.0	1.70	2089	19.58
8	120.0	1.31	1969	19.21
9	120.0	1.31	1974	17.35
10	110.0	2.11	1899	27.25
11	110.0	2.11	1949	23.09
12	110.0	2.11	1989	17.60
13	110.0	1.71	1889	23.12
14	110.0	1.72	1899	21.45
15	110.0	1.72	1914	18.82
16	110.0	1.45	1819	25.50
17	110.0	1.45	1809	14.24
18	110.0	1.32	1769	25.53

As the closed-loop performance of MPC strongly depends on model accuracy, it is important that each model in the bank explains the system dynamics as close as possible. Therefore, the structure of each estimated model, defined by the order of the polynomials $A(q)$, $B(q)$ in (10) is chosen such that the (Root Mean Square Error) RMSE to the experimental data is lower than 20 %. This means that transfer function orders may vary depending on the operating point. At high superheating values (i.e., above 25 K), a first or second order is sufficient to explain the experimental data, however, for lower superheating values, often third or fourth order polynomials A and B are required. In this work, models lower than a 5th order were chosen as increasing further the complexity might not produce general models but instead fall into over-fitting data and/or zero-pole cancellation [59].

Notice that identification signals are applied in open-loop, therefore making more difficult to achieve low superheating values (below 15 K), thus limiting the range of conditions studied, which consequently leads to a lower control performance due to 'higher' modelling error at that extreme condition.

Fig. 6 illustrates how the dynamics of the ORC power unit grow in complexity at lower superheating values, as observed for model 12, identified at $\Delta T_{sh} = 17$ K, which exhibits some extra dynamic behaviour not observed for models 10 and 11, which correspond to higher superheating values.

Such phenomena observed for model 12 in Fig. 6 can be physically explained because of the cycle effect, which is reenforced at low superheating levels. A change (e.g., increase) in the mass flow rate of the working fluid (i.e., pump speed action), affects the operation of the evaporator with a subsequent increment of the heat transfer, varying the saturation temperature and thus leading to a slow but large drop in superheating level (primary effect). This will then change the operation of the condenser, causing a second drop of the superheating level after some delay (i.e., cycle time or time that the fluid takes to return to the evaporator). It is worth mentioning that this effect is also encountered when modelling the system based on first principles as reported in [7], revealing an intrinsic characteristic of the process.

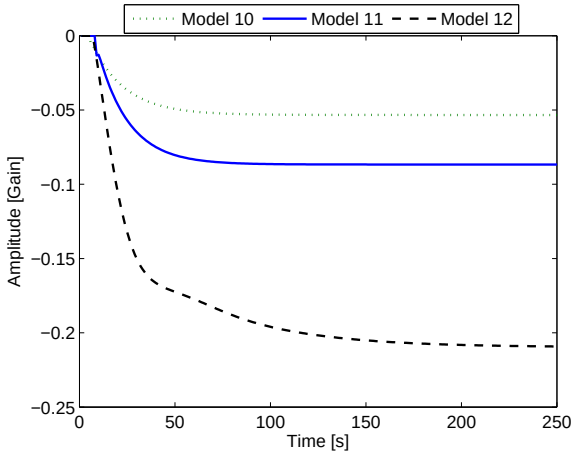

Figure 6: Comparison of the step response for model 12 (dashed black line), model 11 (solid blue line) and model 10 (dotted green line). Secondary or cycle effect present for low superheating values is observed for model 12.

4.2. *Tracking experiment at constant waste heat source conditions*

In order to illustrate the difficulty of controlling superheating level, a single model linear MPC controller is designed and experimentally evaluated for the tracking experiment depicted in Fig. 7, at constant $T_{hf} = 120\,^{\circ}$C and $\dot{m}_{hf} = 1.96$ kg/s in the waste heat source. Main goal is to test the robustness of the controller going closer to the system nonlinearity by decreasing superheating setpoint as close as possible to the $\Delta T_{sh,min} = 10$ K constraint limit.

The single model MPC uses model 5, identified under conditions reported in Table 1, and tuned using $N_p = 60$, $N_c = 1$, $\alpha = 0.5$ and $\lambda = 0$. It is known that a 'smart' choice of the disturbance filter leads to elimination of non-zero average disturbances, perturbations in a specific frequency range and the augmentation of robustness against modelling errors [57, 60]. In this work an integrator has been chosen, leading to zero steady-state error. Other choices are possible if a better knowledge of the frequency content of the waste heat is known as presented in [39].

The controller exhibits a good performance up to a superheating value of 28 K, for further changes in the setpoint the controller starts oscillating until it gets unstable at $\Delta T_{sh} = 23$ K, due to the large prediction error in the controller, making necessary to change to open-loop to bring the system back into a safe

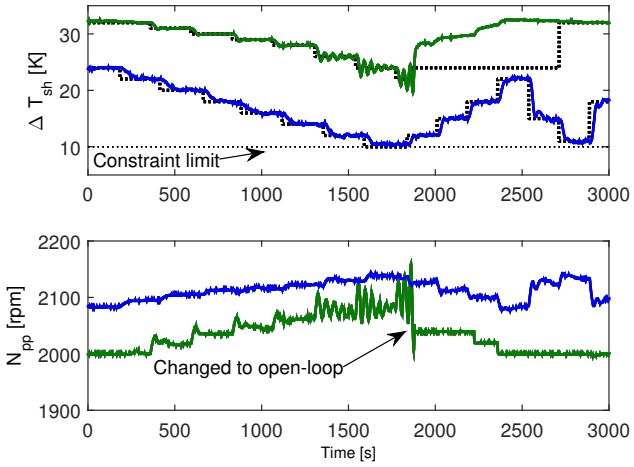

Figure 7: Comparison of the tracking performance of single model MPC (solid green line) and proposed MMPC (solid blue line) strategies for ORC process with constant heat source conditions $T_{hf} = 120\,^{\circ}\mathrm{C}$ and $\dot{m}_{hf} = 1.96\,\mathrm{kg/s}$. Dotted black line represents the setpoint.

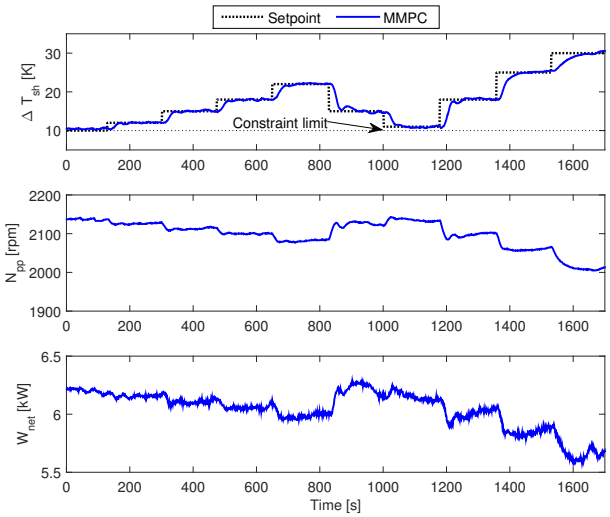

Figure 8: Tracking performance and power produced by MMPC (solid blue line) for large superheating setpoint changes for ORC process with constant heat source conditions $T_{hf} = 120\,^{\circ}\mathrm{C}$ and $\dot{m}_{hf} = 1.96\,\mathrm{kg/s}$.

condition. Next, the MMPC approach is evaluated for a similar tracking experiment, using the tuning parameters $N_p = 60$, $N_c = 1$, $\alpha = 0.5$, $\lambda = 0$, $\psi = 0.055$ and $K = 58$. The controller is able to efficiently track the setpoint changes further below the point where the single model linear MPC became unstable.

System nonlinearity can be observed when analysing the first 1200 s of this test, where nonlinearity rises as previously seen from Fig. 2. Notice that smaller changes in pump speed are required to track the reference at low superheating levels, even when setpoint change for MMPC is the double compared to the 1 K of the single model linear MPC. The multiple model controller can effectively track large reference changes and respects the imposed minimum constraint limit as depicted during the last half part of the experiment, where only small oscillations occur due to the model blending from the Bayes estimator approach (refer to section 4.3).

In order to further test the performance of the proposed MMPC controller, a second tracking experiment is realized. It consists of large superheating setpoint variations (i.e., up to 10 K), which represents a challenge for any controller due to the cycle effect present in ORC power units. As reported in Fig. 8, the controller efficiently follows the setpoint without violating the imposed minimum constraint limit for superheating.

The proposed multiple model controller is clearly able to operate over a wider operating region compared to the linear one. Note that another operating point can be chosen for the linear controller, nevertheless it will be insufficient for the controller to perform efficiently over a wide operating region, leading once more to the conclusion that any sort of robust model adaptation is required. In addition to the previous, the net power ($\dot{W}_{net}$) generated is also plotted in order to verify that for lower superheating values it is possible to increase power production. In this specific test, an increment of 12 % on the output power is obtained by decreasing superheating setpoint while waste heat source conditions remained constant. A small drift in the output power is observed, as temperature in the heat sink rises over time due to external weather conditions.

4.3. *Effect of the Bayesian tuning parameter K*

Another important element to analyse is the effect of the tuning parameter K of the recursive Bayesian weighting scheme, in the closed-loop performance. In order to evaluate this aspect, the Bayesian K parameter is changed on-line while performing a tracking experiment. Three cases are evaluated $K = \{1.8; 18; 58; 75\}$, leading to the results depicted in Fig. 9.

Usually complex dynamics can be better explained when blending the models, i.e., by choosing low K values [44, 61, 45]. This is however true when the models are close to each other. For the studied case, experiments at low superheating degree are difficult to achieve, therefore, it is beneficial to blend less, and instead converge to only two or three prediction combinations.

The previous statement can be verified using results from Fig. 9, where performance for low superheating values is improved by selecting higher K values. On the other hand, selecting even larger values (i.e., larger than 58 for this specific study) might lead to selection of a single model, thus deteriorating the closed-loop performance, since it will behave as a standard single model MPC approach, which has been observed to be insufficient for control of ORC power units.

In order to quantify the closed loop performance over the different K values, three commonly used measures of the tracking error ε are implemented, namely Root Mean Square (RMSE), Integral Absolute Error (IAE) and Integral Time-weighted Absolute Error (ITAE), defined as follows:

$$RMSE = \sqrt{\frac{1}{T}\int_0^T \varepsilon^2 dt} \tag{29}$$

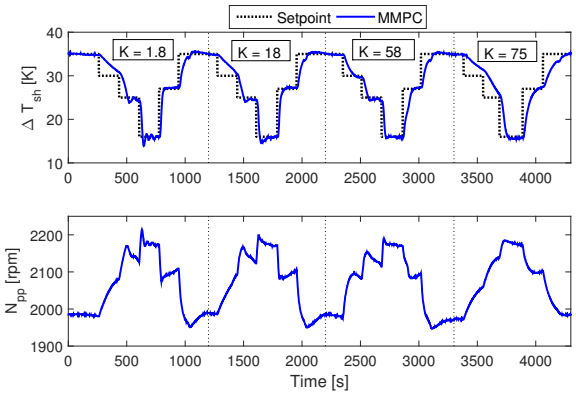

Figure 9: Assessment of the influence of tuning K matrix in MMPC tracking performance of ORC process with constant heat source conditions $T_{hf} = 120\,^{\circ}\mathrm{C}$ and $\dot{m}_{hf} = 1.96\,\mathrm{kg/s}$.

$$IAE = \int_0^T |\varepsilon| dt \tag{30}$$

$$ITAE = \int_0^T t|\varepsilon| dt \tag{31}$$

The results obtained are reported in Table 2. The RMSE can here be understood as a measure of the imperfection of the controller to follow the reference, an indication of the variance, since it penalizes large errors more than smaller ones (i.e., the square of a large error will be much bigger). Therefore it is expected that controller tuned with minimum RMSE is the one which is expected to eliminate large errors quicker. Based on this perspective, $K = 18$ represents the best choice, which can be verified as it better tracks the reference producing the lowest error. This criterion indicates that controller $K = 18$ is also the fastest.

The IAE criterion does not add weight to any of the errors in the system response, it indicates the controller with best tracking performance without penalizing transient; from this perspective $K = 58$ represents the best choice, as it exhibits the lowest overall error. ITAE weights errors which exist after a long time much more heavily than those at the start of the response, thus it might illustrate which controller settles without oscillations, it is therefore not a good representation for systems with sluggish initial response; in this aspect $K = 58$ represents once more the best choice as it settles without overshoot.

Previous analysis suggests that either 18 or 58 are good values for K tuning parameter, nevertheless, by considering that the latter presents less undershoot (see Fig. 9), this is preferred. Having a lower undershoot might be beneficial as it allows to operate closer to the constraint limits, even when the reference decreases as observed from Fig. 8 and Fig. 9. Notice that for all performance indexes $K = 75$ performs the worst, thus indicating that there exists, for this specific case study, an optimal value in between $K = 18$ and $K = 75$. How to precisely optimise this choice is out of the scope of this article, but it appears as an interesting topic for future research.

Table 2: Performance indexes for Bayesian tuning parameter K.

K	RMSE	IAE	ITAE
1.8	2.77	1668	27.8x10^6
18	**2.68**	1581	26.4x10^6
58	2.74	**1484**	**25.0**x10^6
75	3.42	2163	32.0x10^6

4.4. Tracking and disturbance rejection performance

Up to now, evaluation of the closed-loop performance has been restricted to constant waste heat source conditions, which is an unrealistic scenario due to its inherently fluctuating nature. Hence, an additional experiment is performed where T_{hf} and $\dot{m}_{hf}$ vary over a wide range of conditions. Fluctuations are large in amplitude and fast, as encountered in the most challenging industrial waste heat conditions [46].

The experimental results depicted in Fig. 10 show the effectiveness of the MMPC controller to efficiently compensate the sudden disturbances created by the waste heat fluctuations. The controller tracks the given setpoint variations, while respecting the imposed input and output constraints. In order to quantify the capacity of the controller to reject the disturbances, the root mean square is computed on the tracking error during the period from 800 s to 1900 s, where setpoint is constant and the controller is exposed to heat source variations of $T_{hf} = 110 \pm 8\,^{\circ}\mathrm{C}$ and $\dot{m}_{hf} = 1.8 \pm 0.3\,\mathrm{kg/s}$, giving as result $RMSE = 1.31\,\mathrm{K}$, meaning that an output variance lower than 2 K is observed for superheating, despite the drastic changes of the waste heat source. The controller keeps the system safe and stable even when setpoint is reduced to 15 K, as illustrated during the period from 2050 s to 2200 s, where the root mean square on the tracking error is $RMSE = 0.52\,\mathrm{K}$.

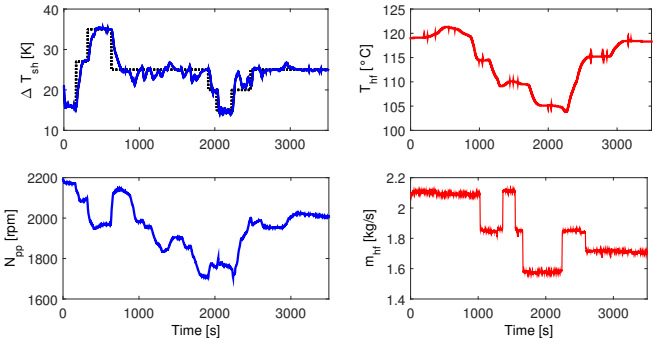

Figure 10: Assessment of the disturbance rejection capabilities of the proposed MMPC for ORC process with large waste heat source variations in both temperature T_{hf} and mass flow rate $\dot{m}_{hf}$.

An additional test is performed for waste heat conditions presented in Fig. 11, where T_{hf} and $\dot{m}_{hf}$ vary within a bandwidth of 5 mHz and amplitude changes as high as possible into the pilot plant physical limits. The main target here is to keep superheating as close as possible to setpoint, i.e., testing regulation capabilities of the controller.

The experimental results obtained show that for the case of variations in the thermal energy source, a characteristic of waste heat recovery applications, the control performance is not substantially deteriorated when decreasing the setpoint from 25 K close to 18 K, since RMSE tracking error reported is 0.85 K and 1.26 K, respectively. More importantly, when comparing the power production, it is encountered that system operating at the lowest superheating produced about 6 % more net electrical energy, as already noticed from Fig. 8. This result is close to the expected performance reported by simulation studies in recent literature, where it is stated that by an accurate superheating regulation, it is possible to operate the system closer to the optimal conditions even for large variations in the waste heat source, thus leading to an enhanced cycle performance, maximizing the output power [3].

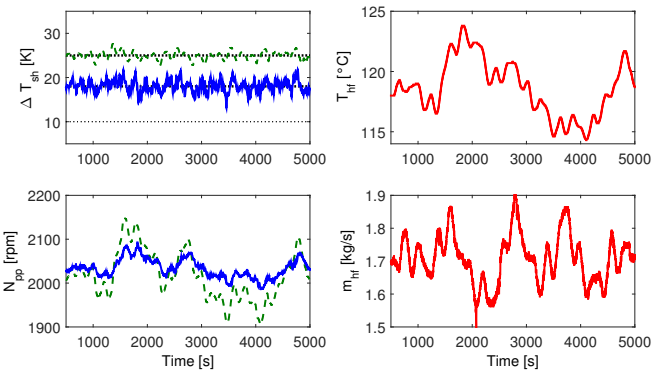

Figure 11: Assessment of the disturbance rejection capabilities of MMPC for ORC process with large waste-heat source variations in both temperature and mass flow rate for 'high' and 'low' superheating setpoint values.

The proposed control strategy can be applied to real applications, by implementing the following procedure: 1) identify the temperature and mass flow rate range of the waste heat source (i.e., define a minimum and a maximum), 2) use system identification techniques to model the superheating degree dynamics, for the four extreme waste heat source conditions, paying special attention to the case of low temperature and low mass flow rate as nonlinearity is dominant in these conditions , 3) define other intermediate operating points to model the system in order to have enough models in the bank, a minimum of 12 models should be obtained (i.e., three models at high, intermediate and low superheating degree for each pair of extreme waste heat source conditions), 4) implement the MMPC algorithm and perform initial tests at 'high' superheating degree in order to tune the Bayesian K tuning parameter, 5) perform additional test at lower superheating degrees to verify the closed-loop performance.

5. Conclusions

In this contribution an efficient control strategy for regulation of superheating in a 11 kW_{el} organic Rankine cycle pilot plant employed for waste heat recovery is presented. The proposed control strategy is a Multiple Model Predictive Controller able to deal with systems with time-varying nonlinear dynamics.

Since the challenge in control design for organic Rankine cycle units comes from the superheating degree due to its nonlinear time-varying characteristic, a linear controller proved to be insufficient to properly operate the ORC system over a wide range of conditions. On the other hand, the experimental study illustrates that the multiple model predictive control approach allows to safely reach low superheating degree, thus making possible to increase the produced output power up to 6 %, even when large temperature and mass flow variations in the heat source are applied. The proposed algorithm probes to be efficient to deal with fast and large amplitude waste heat fluctuations as those encountered on some industrial applications, while keeping the superheating degree below 2 K when measuring the root mean square of the tracking error. Compared to other multiple-model predictive controllers found in literature (e.g., [44, 30]) which combine the models based on a weighting scheme, the proposed controller takes advantages of the filtering techniques used for prediction, allowing to use different model structures in the bank without increasing complexity of the optimisation problem, and thus is not strictly limited to the use of First Order plus Time Delay transfer functions. An additional advantage concerns the recursive Bayesian weighting scheme, as it allows to use a large list of candidates inside the bank of models, without increasing substantially the computation time, by rejecting poor models exponentially fast. Moreover, by using the small cut-off probability, it is possible to keep alive all models inside the bank. The tuning K parameter allows to choose between blending more predictions, when choosing low K values, or to converge to a single model prediction, for large K values. For this studied case 'large' values in K are preferred, since blending predictions will lead to larger modelling errors. The multiple model strategy keeps a similar filtering approach as in single model model predictive control for noise and disturbance prediction, hence avoiding the use of Diophantine equations or observer design, making it suitable for implementation on commonly used industrial hardware.

Future work includes to extend the methodology for the multiple-input multiple-output case, in order to use expander speed as an additional degree of freedom; and the development of a method to optimise the choice of the Bayesian tuning K matrix.

Acknowledgments

The results presented in this paper have been obtained within the frame of the IWT SBO-110006 project The Next Generation Organic Rankine Cycles (www.orcnext.be), funded by the Institute for the Promotion and Innovation by Science and Technology in Flanders, Belgium. This financial support is gratefully acknowledged. We declare that there is no conflict of interest.

References

[1] IEA, Industrial excess heat recovery technologies & applications, Tech. rep., Technical report, Industrial Energy-related Technologies and Systems (IETS) (2014).

[2] C. Carcasci, R. Ferraro, E. Miliotti, Thermodynamic analysis of an organic rankine cycle for waste heat recovery from gas turbines, Energy 65 (2014) 91 – 100. doi:http://dx.doi.org/10.1016/j.energy.2013.11.080.

[3] S. Quoilin, M. Van Den Broek, S. Declaye, P. Dewallef, V. Lemort, Techno-economic survey of organic rankine cycle (orc) systems, Renewable and Sustainable Energy Reviews 22 (2013) 168–186. doi:10.1016/j.rser.2013.01.028.

[4] I. Obernberger, P. Thonhofer, E. Reisenhofer, Description and evaluation of the new 1000kwel organic rankine cycle process integrated biomass chp plant in lienz, austria, Euroheat and Power 10 (2002) 1–17.

[5] S. Quoilin, M. Orosz, H. Hemond, V. Lemort, Performance and design optimization of a low-cost solar organic rankine cycle for remote power generation, Solar Energy 85 (5) (2011) 955 – 966. doi:http://dx.doi.org/10.1016/j.solener.2011.02.010.

[6] L. Guillaume, A. Legros, A. Desideri, V. Lemort, Performance of a radial-inflow turbine integrated in an orc system and designed for a whr on truck application: An experimental comparison between r245fa and r1233zd, Applied Energy 186, Part 3 (2017) 408 – 422, sustainable Thermal Energy Management (SusTEM2015). doi:http://dx.doi.org/10.1016/j.apenergy.2016.03.012.

[7] S. Quoilin, R. Aumann, A. Grill, A. Schuster, V. Lemort, Dynamic modeling and optimal control strategy for waste heat recovery organic rankine cycles, Applied Energy Vol. 88 (2011) 2183–2190.

[8] H. Jouhara, N. Khordehgah, S. Almahmoud, B. Delpech, A. Chauhan, S. A. Tassou, Waste heat recovery technologies and applications, Thermal Science and Engineering Progress 6 (2018) 268 – 289. doi:https://doi.org/10.1016/j.tsep.2018.04.017.

[9] H. Xie, C. Yang, Dynamic behavior of rankine cycle system for waste heat recovery of heavy duty diesel engines under driving cycle, Applied Energy 112 (2013) 130 – 141. doi:http://dx.doi.org/10.1016/j.apenergy.2013.05.071.

[10] M. Bakosova, J. Oravec, Robust model predictive control for heat exchanger network, Applied Thermal Engineering 73 (1) (2014) 924 – 930. doi:https://doi.org/10.1016/j.applthermaleng.2014.08.023.

[11] M. Imran, R. Pili, M. Usman, F. Haglind, Dynamic modeling and control strategies of organic rankine cycle systems: Methods and challenges, Applied Energy 276 (2020) 115537. doi:https://doi.org/10.1016/j.apenergy.2020.115537.

[12] J. Sun, W. Li., Operation optimization of an organic rankine cycle (orc) heat recovery power plant, J. Applied Thermal Engineering Vol. 31 (2011) 2032–2041.

[13] S. Lecompte, H. Huisseune, M. van den Broek, M. D. Paepe, Methodical thermodynamic analysis and regression models of organic rankine cycle architectures for waste heat recovery, Energy 87 (2015) 60 – 76. doi:http://dx.doi.org/10.1016/j.energy.2015.04.094.

[14] F. Casella, T. Mathijssen, P. Colonna, J. Van Buijtenen., Dynamic modeling of organic rankine cycle power systems, Journal of Engineering for Gas Turbines and Power Vol 135 (2013) 042310–042310–12.

[15] A. Desideri, A. Hernandez, S. Gusev, M. van den Broek, V. Lemort, S. Quoilin, Steady-state and dynamic validation of a small-scale waste heat recovery system using the thermocycle modelica library, Energy 115, Part 1 (2016) 684 – 696. doi:http://dx.doi.org/10.1016/j.energy.2016.09.004.

[16] V. Grelet, T. Reiche, V. Lemort, M. Nadri, P. Dufour, Transient performance evaluation of waste heat recovery rankine cycle based system for heavy duty trucks, Applied Energy 165 (2016) 878 – 892. doi:http://dx.doi.org/10.1016/j.apenergy.2015.11.004.

[17] V. Grelet, P. Dufour, M. Nadri, T. Reiche, V. Lemort, Modeling and control of rankine based waste heat recovery systems for heavy duty trucks, IFAC-PapersOnLine 48 (8) (2015) 568 – 573, 9th IFAC Symposium on Advanced Control of Chemical Processes (ADCHEM'15). Whistler, Canada. doi:http://dx.doi.org/10.1016/j.ifacol.2015.09.028.

[18] A. Hernandez, A. Desideri, C. Ionescu, S. Quoilin, V. Lemort, R. De Keyser, Increasing the efficiency of organic rankine cycle technology by means of multivariable predictive control, IFAC Proceedings Volumes 47 (3) (2014) 2195 – 2200, 19th IFAC World Congress. doi:http://dx.doi.org/10.3182/20140824-6-ZA-1003.01796.

[19] E. Feru, F. Willems, B. de Jager, M. Steinbuch, Modeling and control of a parallelwaste heat recovery system for euro-vi heavy-duty diesel engines, energies 7 (2014) 6571–6592.

[20] J. Peralez, P. Tona, M. Nadri, P. Dufour, A. Sciarretta, Optimal control for an organic rankine cycle on board a diesel-electric railcar, Journal of Process Control 33 (2015) 1 – 13.

[21] P. Tona, J. Peralez, Control of organic rankine cycle systems on board heavy-duty vehicles: a survey, IFAC-PapersOnLine 48 (15) (2015) 419 – 426. doi:http://dx.doi.org/10.1016/j.ifacol.2015.10.060.

[22] J. Peralez, M. Nadri, P. Dufour, P. Tona, A. Sciarretta, Organic rankine cycle for vehicles: Control design and experimental results, IEEE Transactions on Control Systems Technology 25 (3) (2017) 952–965. doi:10.1109/TCST.2016.2574760.

[23] D. Wei, X. Lu, Z. Lu, J. Gu, Performance analysis and optimization of organic rankine cycle (orc) for waste heat recovery, J. Energy Conversion and Management Vol. 48 (2007) 1113–1119.

[24] A. Hernandez, A. Desideri, C. Ionescu, R. De Keyser, V. Lemort, S. Quoilin, Real-time optimization of organic rankine cycle systems by extremum-seeking control., (Energies) 9(5):334.

[25] A. Hernandez, A. Desideri, C. Ionescu, S. Quoilin, V. Lemort, R. De Keyser, Towards the optimal operation of an organic rankine cycle unit by means of model predictive control, in: 3rd International Seminar on ORC Power Systems (ASME ORC 2015), 2015.

[26] A. Hernandez, F. Ruiz, A. Desideri, C. Ionescu, S. Quoilin, V. Lemort, R. De Keyser, Nonlinear identification and control of organic rankine cycle systems using sparse polynomial models, in: 2016 IEEE Conference on Control Applications (CCA), 2016, pp. 1012–1017. doi:10.1109/CCA.2016.7587946.

[27] D. Wei, X. Lu, Z. Lu, J. Gu, Dynamic modeling and simulation of an organic rankine cycle (orc) system for waste heat recovery, Applied Thermal Engineering 28 (10) (2008) 1216 – 1224. doi:https://doi.org/10.1016/j.applthermaleng.2007.07.019.

[28] J. Galindo, V. Dolz, L. Royo-Pascual, A. Brizard, Dynamic modeling of an organic rankine cycle to recover waste heat for transportation vehicles, Energy Procedia 129 (2017) 192 – 199, 4th International Seminar on ORC Power Systems, September 13-15th, Italy. doi:https://doi.org/10.1016/j.egypro.2017.09.111.

[29] J. Zhang, M. Lin, F. Fang, J. Xu, K. Li, Gain scheduling control of waste heat energy conversion systems based on an {LPV} (linear parameter varying) model, Energy 107 (2016) 773 – 783. doi:http://dx.doi.org/10.1016/j.energy.2016.04.064.

[30] V. Grelet, P. Dufour, M. Nadri, V. Lemort, T. Reichel, Explicit multimodel predictive control of a waste heat rankine based system for heavy duty trucks, in: In IEEE Conference on Decision and Control, Osaka, Japan, 2015.

[31] J. Zhang, T. Zhang, M. Lin, G. Hou, K. Li, Multiple model predictive control for organic rankine cycle (orc) based waste heat energy conversion systems, in: 2016 UKACC 11th International Conference on Control, 2016, pp. 1–7. doi:10.1109/CONTROL.2016.7737577.

[32] H. Koppauer, W. Kemmetmüller, A. Kugi, Model predictive control of an automotive waste heat recovery system, Control Engineering Practice 81 (2018) 28 – 42. doi:https://doi.org/10.1016/j.conengprac.2018.09.005.

[33] B. Xu, D. Rathod, A. Yebi, Z. Filipi, A comparative analysis of real-time power optimization for organic rankine cycle waste heat recovery systems, Applied Thermal Engineering 164 (2020) 114442. doi:https://doi.org/10.1016/j.applthermaleng.2019.114442.

[34] X. Wu, J. Chen, L. Xie, Fast economic nonlinear model predictive control strategy of organic rankine cycle for waste heat recovery: Simulation-based studies, Energy 180 (2019) 520–534. doi:https://doi.org/10.1016/j.energy.2019.05.023.
URL https://www.sciencedirect.com/science/article/pii/S036054421

[35] V. Grelet, Rankine cycle based waste heat recovery system applied to heavy duty vehicles: topological optimization and model based contro, Ph.D. thesis, Automatic Control Engineering, Universite de Lyon (2016).

[36] X. Liu, A. Yebi, P. Anschel, J. Shutty, B. Xu, M. Hoffman, S. Onori, Model predictive control of an organic rankine cycle system, Energy Procedia 129 (2017) 184 – 191, 4th International Seminar on ORC Power Systems September 13-15th 2017, Milano, Italy. doi:https://doi.org/10.1016/j.egypro.2017.09.109.

[37] D. Seitz, O. Gehring, C. Bunz, M. Brunschier, O. Sawodny, Model-based control of exhaust heat recovery in a heavy-duty vehicle, Control Engineering Practice 70 (2018) 15 – 28. doi:https://doi.org/10.1016/j.conengprac.2017.08.010.

[38] E. Feru, N. Murgovski, B. de Jager, F. Willems, Supervisory control of a heavy-duty diesel engine with an electrified waste heat re-

covery system, Control Engineering Practice 54 (2016) 190 – 201. doi:http://dx.doi.org/10.1016/j.conengprac.2016.06.001.
[39] A. Hernandez, A. Desideri, S. Gusev, C. Ionescu, M. van den Broek, S. Quoilin, V. Lemort, R. De Keyser, Design and experimental validation of an adaptive control law to maximize the power generation of a small-scale waste heat recovery system, Applied Energy 203 (2017) 549–559.
[40] S. Qin, T. Badgwell, A survey of industrial model predictive control technology., Control engineering practice 11 (2003) 733–764.
[41] F. Allgower, R. Findeisen, Z. Nagy, Nonlinear model predictive control: from theory to application, J. Chin. Inst. Chem. Engrs. 35(3) (2004) 299 – 315.
[42] E. F. Camacho, C. Bordons, Model Predictive Control, 2nd Edition, Vol. 405 pages, Springer-Verlag, London,, 2004.
[43] M. L. Darby, M. Nikolaou, Mpc: Current practice and challenges, Control Engineering Practice 20 (4) (2012) 328 – 342, special Section: IFAC Symposium on Advanced Control of Chemical Processes - ADCHEM 2009. doi:http://dx.doi.org/10.1016/j.conengprac.2011.12.004.
[44] B. Aufderheide, B. W. Bequette, Extension of dynamic matrix control to multiple models, Computers and Chemical Engineering 27 (2003) 1079 – 1096. doi:doi:10.1016/S0098-1354(03)00038-3.
[45] R. R. Rao, B. Aufderheide, B. W. Bequette, Experimental studies on multiple-model predictive control for automated regulation of hemodynamic variables, IEEE Transactions on Biomedical Engineering 50 (3) (2003) 277–288. doi:10.1109/TBME.2003.808813.
[46] M. Jimenez-Arreola, R. Pili, F. Dal Magro, C. Wieland, S. Rajoo, A. Romagnoli, Thermal power fluctuations in waste heat to power systems: An overview on the challenges and current solutions, Applied Thermal Engineering 134 (2018) 576–584. doi:https://doi.org/10.1016/j.applthermaleng.2018.02.033.
URL https://www.sciencedirect.com/science/article/pii/S1359431117370710
[47] L. Grune, J. Pannek, Nonlinear Model Predictive Control. Theory and algorithms., Springer, 2011.
[48] E. C. Garcia, Quadratic dynamic matrix control of nonlinear processes, in: Presented at the AIChE annual meeting, San Francisco CA, 1984.
[49] G. Gattu, E. Zafiriou, Nonlinear quadratic dynamic matrix control with state estimation, Industrial and Engineering Chemistry Research 31 (1992) 187 – 202. doi:DOI: 10.1021/ie00004a018.
[50] Z. Zhao, X. Xia, J. Wang, J. Gu, Y. Jin, Nonlinear dynamic matrix control based on multiple operating models, Journal of process control 13 (2003) 41–46.
[51] F. Declercq, R. De Keyser, Suboptimal nonlinear predictive controllers, Int. J. Appl. Math. and Comp. Sci. 9(1) (1999) 129 – 148.
[52] R. De Keyser, Model based Predictive Control for Linear Systems, Invited chapter in UNESCO EoLSS. Oxford (6.43.16.1), 2003.
[53] R. De Keyser, A. Van Cauwenberge, A self-tuning multistep predictor application, Automatica 17(1) (1981) 167 – 174.
[54] R. De Keyser, A. Van Cauwenberge, Epsac: Extended prediction self-adaptive control, in: IFAC symposium on Identification, 1985, pp. 1255 – 1260.
[55] A. Dutta, Design and certification of industrial predictive controllers, Ph.D. thesis, Ghent University (2014).
[56] A. Maxim, D. Copot, R. De Keyser, C.-M. Ionescu, An industrially relevant formulation of a distributed model predictive control algorithm based on minimal process information, Journal of Process Control 68 (2018) 240–253.
URL http://dx.doi.org/10.1016/j.jprocont.2018.06.004
[57] J. Maciejowski, Predictive Control: With Constraints, Pearson Education, Prentice Hall, 2002.
[58] L. Wang, Model Predictive Control System Design and Implementation Using Matlab, Advances in Industrial Control, Springer, 2010.
[59] L. Ljung, System identification: theory for the user, Prentice-Hall, 2007.
[60] R. De Keyser, C. Ionescu, The disturbance model in model based predictive control, in: In Proceedings of IEEE Conference on Control Applications, Vol. 1, 2003, pp. 446–451 vol.1. doi:10.1109/CCA.2003.1223451.
[61] D. Dougherty, D. Cooper, A practical multiple model adaptive strategy for multivariable model predictive control, Control Engineering Practice 11 (6) (2003) 649 – 664. doi:http://dx.doi.org/10.1016/S0967-0661(02)00170-3.